Double-charge model for classical force-field simulations

Christopher Barrett and Lin-Wang Wang

Phys. Rev. B **91**, 235407 — Published 8 June 2015

DOI: 10.1103/PhysRevB.91.235407

Double charge model for classical force field simulations

Christopher Barrett[1,2] and Lin-Wang Wang[2]*

[1]Department of Materials Science and Engineering, University of California, Berkeley, California 94720, USA

[2]Material Sciences Division, Lawrence Berkeley National Laboratory, Berkeley, California 94720, USA

*lwwang@lbl.gov

Date received: October 13th, 2014

Abstract: In a traditional classical force field model, the atomic point charge that generates the electrostatic potential, and the Born charge induced by atomic movement, are represented by the same charge parameter. But their actual values can be very different, and correct values for both of them are needed in order to yield the correct atomic structure (electrostatic charge) and phonon spectrum (Born charge). This is particularly true for nanostructure calculations. Here, we introduce a Double Charge Model (DCM) to reconcile the difference between the electrostatic charge and Born charge. The DCM allows us to reproduce the accurate *ab initio* phonon spectrum not only in bulk systems, but also for nanostructures (slabs and nanowires). This enables the use of classical force fields to study phonon spectra of large nanostructures, which are important for many phenomena from carrier dynamics to thermo conductivities.

PACS: 63.22.-m; 63.20.D-; 62.23.Hj;

There are two common approaches to simulate material properties at the atomic level. One is the *ab initio* quantum mechanical method (e.g., density functional theory (DFT) [1], or quantum chemistry [2]), the other is the classical force field model (e.g., bond-potential models for covalent systems [3], or embedded atom models for metallic systems [4]). Although *ab initio* methods have advanced and popularized in recent years, many problems still are better studied by force field methods, e.g., large biological or organic systems, nanosystems, and molecular dynamics simulations. The achievements of combining classical force field and quantum chemistry methods have been exemplified recently by the awarding of the Nobel Prize to three of its pioneers in 2013. Force field development is still an active research field. One example is the reactive force field development, which incorporates the bond breaking and forming during chemical reactions [5]. Another is the charge model, which often determines the accuracy of the potential, and is the focus of this study. In a force field [3], the atom-atom interaction is divided into two parts: the chemical bonding part, and the non-bonding part, which

includes the van der Waals interactions and electric charge interactions. Beyond the point-charge model, the current development of charge models focuses mostly on the point charge dipole, and the related point charge polarizability on each atom [6]. However, there is another problem that has been overlooked. That is, the Born effective charge (BEC) tensor [7], which describes how the electric dipole changes when a nucleus moves, can have amplitudes much larger than the point charge obtained by fitting the molecular electrostatic potential [8]. This is a serious problem for nanostructure simulations. To predict correct atomic structures, the correct electrostatic charge is needed, and to predict the correct phonon spectra, which is the concern of this study, the correct BEC is needed (e.g., to get the correct longitudinal optical (LO) and transverse optical (TO) phonon splitting in a bulk [9]). Unfortunately, in a simple atomic point-charge model, these two are the same, both equal to the atomic point charge, and this cannot be resolved by any polarization model mentioned above. In this work, we introduce a new point charge model to any classical force field, which reconciles the BEC with the electrostatic charge. We call this the Double Charge Model (DCM) since it assigns two charges on each atom. We apply this model to nanostructure simulations. The goal of the force field is not just to relax the atomic positions of large nanostructures, but to calculate their phonon spectra. Although there are many previous calculations of quantum dot phonon modes [10, 11, 12], they all involve crude treatment of the surface passivation, thus their surface-related phonon modes are not reliable. The development of the DCM allows us to elevate such calculations to a new level where the *ab initio* surface phonon modes can also be accurately reproduced. Accurate calculation of nanosystem phonon spectra is important for many studies, e.g., to calculate their thermo conductivity, or to study hot carrier relaxation through electron-phonon coupling. Since these systems are often beyond direct *ab initio* calculations, we expect the DCM can be used for such studies in the future.

While there are many force field models for organic systems [13-18], here we will focus on the Valence Force Field (VFF) model originally developed by Keating [19] for solid state calculations. The general VFF model can be written as:

$$E_b = \frac{1}{2}\sum_i \sum_j^{nn(i)} \frac{3\alpha_{ij}}{8(d_{ij}^0)^2}\left[R_{ij}^2 - \left(d_{ij}^0\right)^2\right]^2 + \frac{1}{2}\sum_i \sum_{j,k\neq j}^{nn(i)} \frac{3\beta_{i,jk}}{8d_{ij}^0 d_{ik}^0}\left[R_{ji} \bullet R_{ki} - \cos(\theta_{i,jk}^0) d_{ij}^0 d_{ik}^0\right]^2$$

$$+ \sum_i \sum_{j,k\neq j}^{nn(i)} \left\{ \frac{3\gamma_{i,j,k}}{8d_{ij}^0 d_{ik}^0}\left[R_{ji} \bullet R_{ki} - \cos(\theta_{i,jk}^0) d_{ij}^0 d_{ik}^0\right]\left[R_{ij}^2 - \left(d_{ij}^0\right)^2\right] + \frac{1}{2}\frac{3\delta_{i,j,k}}{8d_{ij}^0 d_{ik}^0}\left[R_{ij}^2 - \left(d_{ij}^0\right)^2\right]\left[R_{ki}^2 - (d_{ik}^0)^2\right] \right\}$$

$$+ \frac{1}{2}\sum_i \sum_{j,k\neq j}^{nn(i)} \sum_{l\neq i}^{nn(k)} \frac{3\varphi_{i,j,k}}{8d_{ik}^0\sqrt{d_{ij}^0 d_{kl}^0}}\left[R_{ji} \bullet R_{ki} - \cos(\theta_{i,jk}^0) d_{ij}^0 d_{ik}^0\right]\left[R_{ik} \bullet R_{lk} - \cos(\theta_{k,il}^0) d_{ki}^0 d_{kl}^0\right] \qquad \text{Eq.(1)}$$

where i refers to an atom, j and k refer to nearest neighbors of i, l refers to a nearest neighbor of k, R_i is the position of atom i, $R_{ij} = R_i - R_j$, d_{ij}^0 refers to the ideal bond length of atom pair i-j, $\theta_{i,jk}^0$ refers to the ideal angle j-i-k, and α, β, γ, δ, and φ are parameters to be fitted. The five terms in Eq.(1) are bond harmonic, angle harmonic, bond-angle, bond-bond, and angle-angle interaction terms. Contrasted with force fields for organic systems [13-18], this force field doesn't have terms like torsion angle rotations. VFF models of this form have been used to model the bulk diamond phonon spectrum [20], phonon spectra of bulk Si and Ge [21, 22], as well as silicon nanowires by Paul et al. [23]. These, however, are all single-element systems with no need to introduce atomic charges.

For other systems, e.g., III-V or II-VI semiconductor compounds, it is necessary to introduce atomic charges. The simplest charge model is to assign one fixed point charge on each atom. Thus, the long-range electrostatic energy will be described as $E_{cc} = \sum_{i>j} q_i q_j / \epsilon_\infty |R_i - R_j|$, where ϵ_∞ is the high-frequency dielectric constant. For CdSe, which will be studied in this work, we use ϵ_∞=5.8, as given by Gorska et al. [24]. We will note that bulk phonon spectra calculated must additionally account for a "nonanalytic term" in the dynamical matrix [25], which results from a long-range Coulomb interaction of phonon modes that cannot be represented in the finite chosen cell. This nonanalytic term computationally gives rise to the LO-TO splitting at the gamma point and essential singularities in non-isotropic structures, including wurtzite. If E_{cc} is simply added to E_b in Eq.(1), it will exert a compressive stress and the minimum energy structure will no longer be at the ideal bond lengths d^0 and bond angles θ^0. That would be a major drawback for such models since the parameters (d^0, θ^0) would need to be fitted along with the coefficients in Eq.(1). To overcome this, Martin [26] has introduced a linear term to counterbalance the E_{cc} stress: $E_l = \frac{1}{2}\sum_i \sum_j^{nn} \eta_{ij} d_{ij}^0 \left(|R_j - R_i| - d_{ij}^0\right)$, where the summation can run through the nearest neighbor list (e.g., for zinc blend (ZB)), or both first- and second-nearest neighbor lists (e.g., for wurzite (WZ)). By properly adjusting η, for bulk systems, it is possible to maintain the ideal d^0, θ^0 values.

With the above $E_{cc} + E_l$ formalism, Martin [26] generated relatively accurate phonon spectra for bulk ZB structures. We have tested this for ZB CdSe, setting q to be the CdSe Born charge of 2.2 (using the trace average of the BEC tensor) as calculated by Dal Corso et al. [27]. The density functional theory (DFT) calculated phonon spectrum and the force field counterpart are shown in Fig.1(a) and (b), respectively. In the DFT calculation, the generalize gradient approximation (GGA) of the PBE [28] density functional is used, and the projector augmented-wave method is used as implemented by the VASP code [29]. The DFT result in Fig.1(a) is in good agreement with previously published DFT results [27]. The same can be calculated for bulk CdSe WZ, as shown in Fig.2(a) and (b). While the comparisons between Fig.1(a) and (b), and Fig.2(a) and (b), are very good, this force field model fails dramatically for nanostructures. To demonstrate this, we studied CdSe WZ (10-10) surfaces (as shown in Fig.2), with the atomic positions $\{R_0\}$ first calculated using DFT. Using the above force field, $E = E_b + E_{cc} + E_l$, the surface becomes unstable: the atomic positions collapse to a dramatically new and unphysical structure (see Fig.3) due to the imbalance of the linear term E_l caused by the surface truncation. The more fundamental reason for this instability is the overly large Coulomb force from E_{cc} and the unphysical linear term E_l.

In molecular systems, one way to get the electrostatic atomic point charge is to fit the electrostatic potential at the periphery of a molecule [8]. Fig.4 shows the electrostatic potential profiles on a plane 3.6 Å away from the CdSe WZ (10-10) surface, calculated from DFT and the point-charge model using q=2.2. We see that the variation of the force field potential is about 5 times that of the DFT potential. Similar conclusions can be drawn based on the comparison on a vertical plane. This implies the BEC is 5 times larger than the electrostatic atomic charge, yielding a 25-fold overestimation of the electrostatic Coulomb forces on the atoms. This causes the collapse of the surface atomic structure when the electrostatic force is not counter-balanced by the artificial linear term E_l. Note, the plane 3.6 Å away from the surface atoms is used instead of a plane closer to the surface, or a plane cutting through the

atoms. This is to avoid the DFT electron charge density and its local Coulomb potential; those local effects are described by the bonding terms E_b in Eq.(1), instead of the point charge terms of E_{cc}.

To solve the above problem of over estimation of the electrostatic potentials, we introduce the Double Charge Model (DCM), which simultaneously provides the correct BEC and electrostatic potential charge. As illustrated in Fig.5, in this model, there are two point charges associated with one atom: One is q at atomic position R, another is q' with its position at R', which in turn is determined by the positions of the nearest neighbor atoms R_n of atom R. More specifically, $R'=\sum_n C_n R_n$, $\sum_n C_n = 1$, and at the minimum energy structure $\{R_0\}$, R'=R (this uniquely determines C_n for an atom with 4 nearest neighbors). For example, for bulk ZB, C_n=1/4. For bulk CdSe WZ, the C_n differ slightly from 1/4 in order to have R'=R due to its deviation from the ideal WZ structure position. The same formula can be applied to surface atoms, which have only three nearest neighbors, if we treat the average position of all second-nearest neighbor atoms as an additional pseudo-nearest neighbor atom. This formula can be further extended to atoms with less than three bonds if the second nearest neighbor atoms are again used to determine the position of R', this time to define multiple pseudo-nearest neighbor atoms. Obviously this formula can be trivially extended to systems where atoms have five or more nearest neighbors, with the help of symmetry to determine C_n. Thus, besides surface atoms, in principle, this formula can also be used to describe defects in the system. However, since our charge model is based on the VFF model, we do need to assume a bonding topology for a given system. Under this model, at the structure $\{R_0\}$, the electrostatic potential charge for a given atom is q+q', while the BEC is q-q' for the bulk systems, hence we have successfully distinguished these two charges (here we assume q(Cd)=-q(Se), q'(Cd)=-q'(Se)). To see that this is true for the BEC, note that displacing one atom not only changes the position of its q (while the position of its q' remains fixed), it will also displace the q_n' positions R_n' of its nearest neighbor atoms R_n as illustrated in Fig.5. As a result, the total BEC is $q+q_n'=q-q'$. The energy in the DCM includes Coulomb interactions for all q-q, q-q' and q'-q' pairs, except q-q' from the same atom. We use q and q' of a given atom to represent the electron plus the nucleus charge cloud for that given atom. Thus, we will not have a Coulomb interaction between q and q' for a given atom. We can regard such interaction as self-interaction, and the related local Coulomb effects should have already been included in the bonding term of Eq.(1). Thus we now have:

$$E_{DCM} = \frac{1}{2\epsilon_\infty}\sum_{i\neq j}\left\{\frac{q_i q_j}{|R_i-R_j|}+\frac{q'_i q'_j}{|R'_i-R'_j|}+2\frac{q_i q'_j}{|R_i-R'_j|}\right\} \qquad \text{Eq.(2)}$$

For periodic systems, this can be calculated via Ewald summation [30].

In our case, since the electrostatic potential charge is much smaller than the BEC, we can use the approximation q'=-q to simplify the model, hence there will be zero electric potential at the relaxed ground state atomic configuration $\{R_0\}$. Then for bulk CdSe, we have 2q=2.2, the BEC. This has the additional benefit that the structure $\{R_0\}$ of the force field model will have the bond lengths and angels described by the parameters d^0_{ij} and θ^0_{ijk} in Eq.(1) without the linear balancing term. This is extremely useful in force field parameter fitting because the ground-state atomic positions, d^0_{ij}, and θ^0_{ijk} can be read from *ab initio* calculations. With E_{DCM} replacing $E_{cc}+E_I$, the parameters in Eq.(1) are refitted, and the resulting phonon spectra are shown in Fig.1(c) and Fig.2(c). Note that E_{DCM} at $\{R_0\}$ does not exert force

under the approximation q'=-q because there is no net charge. More specifically, the electrostatic force given by Eq.(2) can be defined as: $dE_{DCM}/dR_i = \partial E_{DCM}/\partial R_i|_{R'_j} + \sum_j \partial E_{DCM}/\partial R'_j|_{R_i}\, dR'_j/dR_i$. The first term is the electrostatic force on charge q_i due to all other atoms q_k and q'_k, while the second term is the electrostatic charge on q'_j, where j is the nearest neighbor of i. Since the charge $q_k+q'_k=0$ for all the atoms, and at R_0, $R_k=R'_k$, there is no net charge at any atom, then both term equals zero. Although the atomic force contribution of E_{DCM} is zero, it still contributes significantly to the Hessian matrix (since net charge appears after atomic displacement), and hence to the phonon spectrum. As we can see, the phonon spectrum quality is similar to the original $E_{cc}+E_I$ results.

The biggest advantage of this model comes in its application to surfaces and nanostructures, which are most in need of efficient force-field calculations. We studied the WZ CdSe (10-10) surface, which is self-passivated and has a well-known reconstruction [31], with its relaxed atomic positions calculated by *ab initio* methods, shown in Fig.6(a). Our VFF+DCM procedure then takes the *ab initio* calculated atomic structures and refits the surface-related force parameters. The resulting phonon spectrum for a WZ slab is shown in Fig.6(c), together with the DFT result in Fig.6(b). The phonon modes with 51% of their amplitudes in the outer-most two Cd and Se layers are shown as red lines. As can be seen, not only do we get relatively accurate bulk phonon modes, we also get quantitatively correct surface phonon modes. The major difference comes at low frequency, e.g., below 50 cm^{-1}. The VFF+DCM model yields some acoustic modes with energy lower than that of the DFT result. This difference is mostly due to the bonding term E_b of the bulk VFF model, instead of the charge interaction term. It is a common deficiency of such VFF models to not fit the bulk soft acoustic bands very well, e.g., to produce transverse-acoustic bands along the Γ-K direction too high in energy for the zinc-blende system (Fig.1(b) and Fig.1(c)) while producing too-low band energies around the M point in the wurtzite system (Fig.2(b) and Fig.2(c)). To further evaluate the difference between the DFT and VFF+DCM phonon mode vectors, we have calculated their correlation function as $f(\omega_1,\omega_2) = \sum_{k_1,k_2} \left|\sum_R v_{DFT,k_1}(R) v_{VFF,k_2}(R)\right|^2 \delta(\omega_1-\omega_{DFT}(k_1))\delta(\omega_2-\omega_{VFF}(k_2))$, where k_1, k_2 are phonon mode indices, v_k is the eigenvector of phonon k, and ω(k) is the frequency of phonon k. $f(\omega_1,\omega_2)$ is plotted in Fig.6(d) with a small broadening for the two delta functions. If DFT and VFF+DCM phonon mode vectors and frequencies are exactly the same, all peaks of $f(\omega_1,\omega_2)$ would fall on the $\omega_1=\omega_2$ line. As can be seen in Fig.6(d), they fall close to the $\omega_1=\omega_2$ line, indicating good agreement. Note that the charge is important in getting such a good agreement. If we set the BEC to zero, repeat the fitting process, and use the refitted parameters to generate the ZB bulk phonon spectrum, we get a rather different optical phonon spectrum as shown in Fig.7, qualitatively different from the DFT result.

In the above application of the DCM to surfaces, there is an issue that has been ignored so far, and that is the validity of using the bulk BEC and dielectric constant values at the surfaces. Ideally, the *ab initio* Born charge for atoms at the surface and surface-corrected dielectric constants should be used. In practice, we found that the Born charge tensor for a surface atoms can be highly asymmetric, and can hardly be described by a single scalar charge. The surface-corrected dielectric constant, which should depend on the specific Coulomb interaction atomic pair, can also be extremely complicated. Thus, instead of introducing such overly complicated models, and to keep the spirit of simplicity of the model,

we have used the bulk BEC and dielectric constant values to the surface atoms. Such approximation can be further justified by the two facts: (1) any local effect due to the change of BEC and dielectric constant should be absorbed by the refitting of the surface bonding term parameters of Eq.(1); (2) the main purpose of the charge model is to fix the long-range behavior of the electrostatic potential, to the one embodied in the bulk nonanalytic expression for the LO-TO splitting. Such long range terms come mostly from the bulk electric charge, which has been captured correctly by our model. In the end, the adequacy of the approximation is confirmed by the relative good comparison of the slab DFT phonon modes and VFF+DCM phonon modes as shown in Fig.6.

Obtaining an accurate nanostructure phonon spectrum from a force field is non-trivial, especially if both accurate surface atomic positions and phonon spectra are needed. As mentioned above, Paul et al. [23] have used force fields to calculate the phonon spectra of Si nanowire. But Si is a system where atomic charge is not needed. Fu et al. [10] and Ren et al. [11, 12] have used force fields with point-charge Coulomb interactions to calculate the phonon modes of III-V quantum dots. However, in their treatments, the surface bonds are cut abruptly and surface atoms are not fully relaxed, so the exact features of the surface phonon modes are not described accurately. Kelley [32] has used the Lennard-Jones pair potential fit by Rabani [33] to calculate the phonon spectrum of CdSe quantum dots. While this pair potential produces the correct CdSe bulk crystal structure, there is no guarantee its phonon spectrum is accurate even for the bulk. Lin et al. [35] have conducted a comparison between the Rabani force field (including Lennard-Jones and Coulombic terms) to the Tersoff force field (including two- and three-body terms but no charge model at all) for CdSe structures. They conclude that both models produce similar-quality results for the bulk, although they sometimes produce opposite results relative to experiment (for example, the LO/TO frequency ratio), while the Tersoff potential is preferable for nanocrystals. The Rabani force field [33] can produce unphysically drastic atomic rearrangement at the surface. Along this line, Han and Bester [34] have introduced three-body terms on top of the pair potentials to fit the bulk phonon spectra. But even in that case, there is no guarantee that surface atomic positions and surface phonon modes are accurate. In contrast with all of these models, the VFF+DCM has the advantage that it can take the *ab initio* calculated atomic positions to determine the d_{ij}^0 and $\theta_{i,jk}^0$ in Eq.(1), thus only the force constants need to be fit with no need for subsequent relaxation. The drawback, however, is that we can only study well-understood surfaces. Nevertheless, so far, we are not aware of other works where *ab initio* surface phonon modes have been accurately reproduced by a force field model. Furthermore, recent advances enable us to accurately know more about the atomic structures of surface passivations for many nanostructures [36]. Note that, in the fitting procedure, ab initio calculations need to be used to determine the atomic structures of some prototype surfaces. But in actual applications of the VFF+DCM to nanostructures, there is no need to use ab initio calculations. The atomic positions of such nanostructures may be obtained through the VFF+DCM, by minimizing the structures' total energies when necessary.

The true purpose of developing the VFF+DCM is for large nanostructure calculations that are too expensive using *ab initio* methods. Figure 8 shows the phonon spectrum of a nanowire, 26 Å in diameter, with model parameters taken from the slab fitting. While its unit cell only has 108-atoms, to yield the dynamical matrix an 864-atom system is used, corresponding to 8 unit cells in its z direction.

Figure 8 reveals some interesting features. The produced phonon spectrum has no imaginary frequencies, indicating the nanowire structure constructed from slab surface atomic positions is stable under the VFF+DCM model. The highest frequency mode is a surface mode, similar to the top mode found in the slab (Fig.6(c)). This mode corresponds to adjacent surface cadmium and selenium atoms moving in opposite directions in the plane perpendicular to the axis of the wire. This mode is animated in the supplemental materials. Besides this and similar modes, the surface modes have a relatively small contribution to the optical mode spectrum of the wire. On the other hand, there is a large surface contribution to the lower branch of the acoustic phonon modes. Furthermore, there is one single surface dominated phonon mode whose frequency approaches zero at the Γ point. At the gamma point, this mode corresponds to rotation of the nanowire about its axis. Strictly speaking, this is not a surface mode, although it does have the largest amplitudes at the surface. Similar unique far-infrared modes for nanostructures have been observed experimentally for CdSe quantum dots [37]. Such modes can be described using macroscopic continuous elastic models [37]. The phonon modes shown in Fig.8, coupled with its electronic structure calculation, e.g. by charge patching method [38], could be used to study nanostructure carrier transport and carrier cooling in the future.

In conclusion, we have introduced a Double Charge Model to describe the Coulomb interaction within a classical force field model. Such a model can be used to provide the correct charge values for electrostatic potentials and the Born effective charges. While the electrostatic potential is important for atomic relaxation, the Born effective charge is important for the phonon modes. The implementation of the DCM provided both a stable atomic structure and a good phonon spectrum for the surface compared to the DFT results, which were not both attainable using traditional charge models. For the first time, accurate phonon spectra of large nanostructures are available. The calculation of such phonon spectra will not only enable the study electron-phonon interactions, but also allow one to study phonon dynamics and heat transportation in such systems. Finally, the DCM should also be applicable to general classical force field models, e.g. the ones used for organic and biological systems.

Acknowledgment: This work was supported through the Theory of Material project by the Director, Office of Science (SC), Basic Energy Science (BES)/Materials Science and Engineering Division (MSED) of the U.S. Department of Energy (DOE) under the contract No. DE-AC02-05CH11231. It uses the resources of National Energy Research Scientific Computing center (NERSC) supported by the U.S. Department of Energy.

References

[1] P. Hohenberg and W. Kohn, Phys. Rev. **136**, B864 (1964).
[2] P. W. Atkins and R. Friedman, *Molecular Quantum Mechanics* (4th ed.), (Oxford University Press, 2005).
[3] S. J. Weiner, et al., J. Amer. Chem. Soc. **106**, 765 (1984).
[4] M. S. Daw and M. I. Baskes, Phys. Rev. B **29**, 6443 (1984).

[5] A. C. van Duin, S. Dasgupta, F. Lorant, and W.A. Goddard, J. Phys. Chem. A **105**, 9396 (2001).
[6] S. Patel and C.L. III Brooks, J. Comput. Chem. **25**, 1 (2004).
[7] X. Gonze and C. Lee, Phys. Rev. B **55**, 10355 (1997).
[8] T. R. Stouch and D.E. Williams, J. Comp. Chem. **14**, 858 (1993).
[9] P. Y. Yu and M. Cardona, "Fundamentals of Semiconductors" (3rd Ed) (Springer-Verlag, Berlin, Heidelberg, New York, 2001).
[10] H. Fu, V. Ozoliņš, and A. Zunger, Phys. Rev. B **59**, 2881-2887 (1999).
[11] S.-F. Ren, D. Lu, and G. Qin, Phys. Rev. B **63**, 195315 (2001)
[12] S.-F. Ren, Z.-Q. Gu, and D. Lu, Solid State Comm. **113**, 273 (2000)
[13] N. L. Allinger, J. Am. Chem. Soc. **99**, 8127 (1977).
[14] T. Schauman, W. Braun, and K. Wutrich, Biopolymers **29**, 679 (1990).
[15] A. Warshel and S. Lifson, J. Chem. Phys. **53**, 582 (1970).
[16] W. D. Cornell, et al., J. Am. Chem. Soc. **117**, 5179 (1995).
[17] B. R. Brooks, et al., J. Comp. Chem. **4**, 187 (1983).
[18] M. Mollhoff and U. Sternberg, J. Mol. Model. **7**, 90 (2001).
[19] P. N. Keating, Phys. Rev. **145**, 637-645 (1966).
[20] H. L. McMurray, A. W. Solbrig, J. K. Boyter, and C. Noble, J. Phys. Chem. Solids **28**, 2359
[21] R. Tubino, L. Piseri, and G. Zerbi, J. Chem. Phys. **56**, 1022 (1972)
[22] Z. Sui and I. P. Herman, Phys. Rev. B **48**, 17938-17953 (1993).
[23] A. Paul, M. Luisier, and G. Klimeck, J. Comput. Electron. **9**: 160-172 (2010).
[24] M. Gorska and W. Nazarewicz, Phys. Status Solidi (b) **65** (1974) 193
[25] M. Born and K. Huang, *Dynamic Theory of Crystal Lattices* (Clarendon Press, Oxford, 1954), Sec. 30
[26] R. M. Martin, Phys. Rev. B **1**, 4005-4011 (1970).
[27] A. Dal Corso, S. Baroni, R. Resta, and S. de Gironcoli, Phys. Rev. B **47**, 3588 (1993)
[28] J.P. Perdew, K. Burke, and M. Ernzerhof, Phys. Rev. Lett. **77**, 3865 (1996).
[29] G. Kresse and J. Furthmüller, Phys. Rev. B, **54**:11169 (1996).
[30] P. P. Ewald, Ann. Phys. **369**, 253–287 (1921)
[31] L. Manna, L. W. Wang, R. Cingolani, and A. P. Alivisatos, J. Phys. Chem. B **109**, 6183 (2005)
[32] A. M. Kelley, ACS Nano **5**, 5254 (2011)
[33] E. Rabani, J. Chem. Phys. **116**, 258 (2002).
[34] P. Han and G. Bester, Phys. Rev. B **83**, 174304 (2011)
[35] C. Lin, D. F. Kelley, M. Rico, and A. M. Kelley, ACS Nano **8**, 3928 (2014)
[36] D. Zherebetskyy, et al., Science **344**, 1380 (2014).
[37] M.I. Vasilevskiy, et al., Phys. Stat. Sol. B **224**, 2 (2001).
[38] J. Li and L.W. Wang, Phys. Rev. B **72**, 125325 (2005).
See Supplemental Material at [URL will be inserted by publisher] for: a movie of the atomic motions of the highest-frequency phonon mode in the CdSe WZ nanowire modeled by VFF+DCM.

Figures

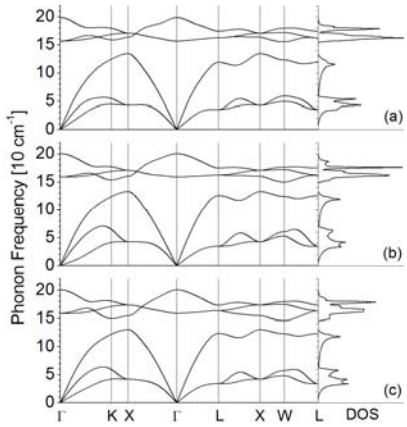

FIG. 1. Phonon dispersion relations in high-symmetry directions, with accompanying density of states plots, for bulk zinc-blende CdSe. (a) VASP GGA DFT. (b) VFF using BECs as atomic charges with linear terms. (c) VFF+DCM.

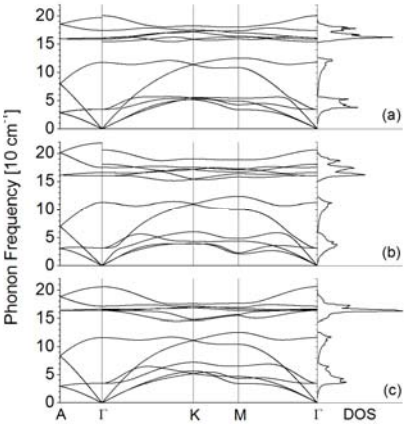

FIG. 2. Phonon dispersion relations in high-symmetry directions, with accompanying density of states plots, for bulk wurtzite CdSe. (a) VASP GGA DFT. (b) VFF using BECs as atomic charges with linear terms. (c) VFF+DCM.

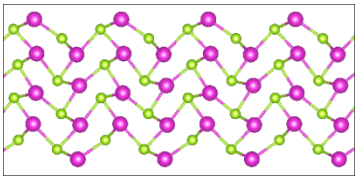

FIG. 3. The quasistable atomic structure of the WZ slab with (10-10) surfaces after relaxation under VFF using the BECs as atomic charges with linear balancing terms. This structure should be compared with the correct structure shown in Fig.6(a). If the mirror symmetry (into the viewing plane shown here) at each atom is broken via a tiny displacement for any atom, the structure will relax further and become completely unstable.

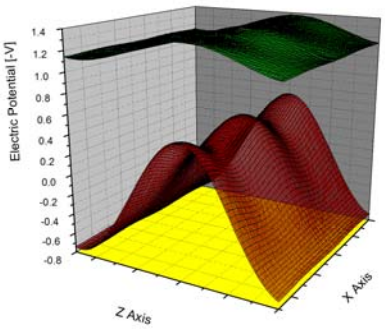

FIG. 4. Surface plots representing the electrostatic potential felt by an electron approximately 3.6 Angstoms above the surface of a CdSe slab, VASP results plotted in green and results from BECs as atomic charges in red. The unit cell of the slab is doubled along the x axis, with the positions of the peaks in both plots corresponding to points in the plane above the surface selenium atoms.

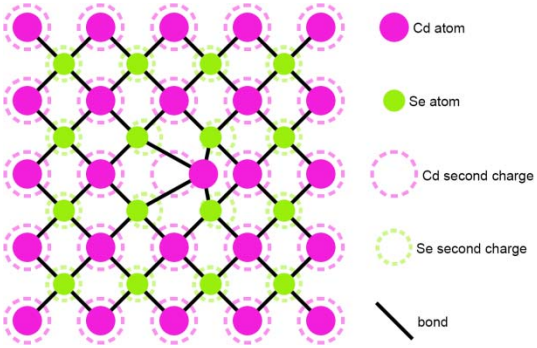

FIG. 5. A cartoon of the DCM applied to a zinc-blende CdSe supercell with a single cadmium atom displaced. The second charge associated with that cadmium atom (purple dashed circle) remains unmoved while the second charges of the four neighboring selenium atoms (green dashed circles) are displaced by one fourth of the cadmium atom's displacement. All other atoms' second charges remain unmoved.

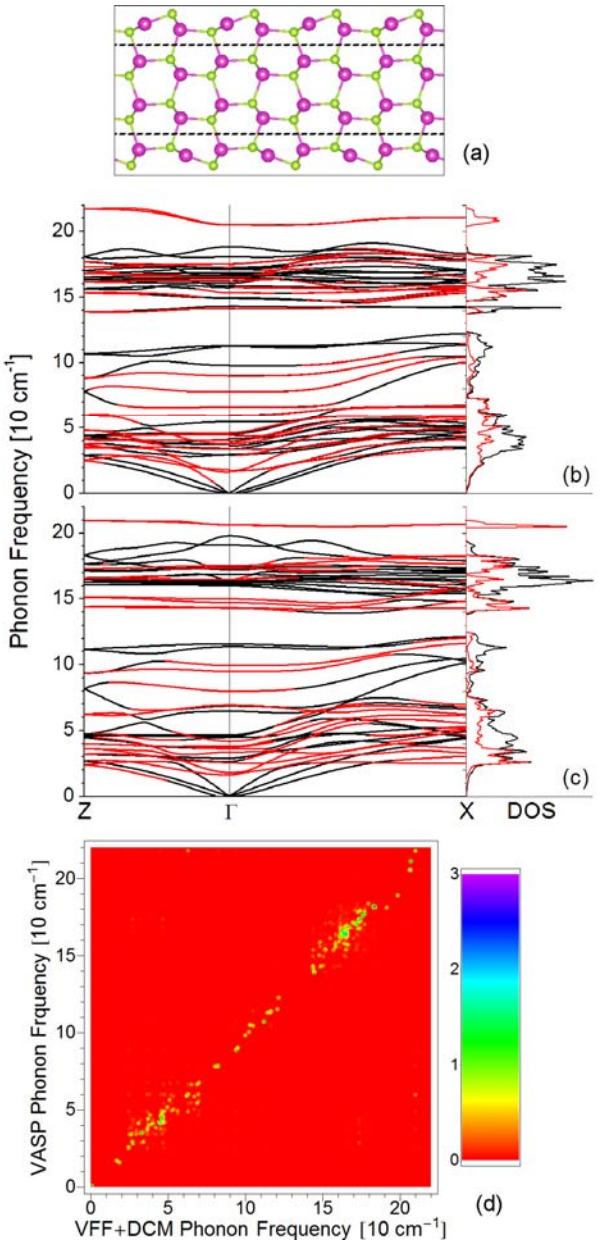

FIG. 6. (a) An isometric view of the wurtzite CdSe slab atomic structure with (10-10) surfaces, viewed down the (0100) direction. Cadmium atoms are represented in purple, selenium atoms in green. The Z-Γ direction is along the horizontal direction in (a), The Γ-X direction is into the plane (both in reciprocal space). (b), (c) Phonon dispersion relations in high-symmetry directions, with accompanying density of states (DOS) plots, for the slab in (a): (b) DFT; (c) VFF+DCM. Phonon eigenstates to which the outermost two layers of atoms (dashed line in (a)) contribute at least 51% are colored in red, both in the dispersion and DOS. The black line in DOS is the total DOS. (d) The correlation function $f(\omega_1,\omega_2)$ which tests the phonon frequencies and phonon mode vectors, plotted here for the Z, Γ, and X points (see text for definition).

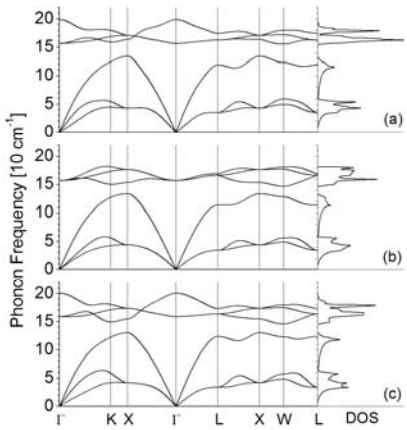

FIG.7. Phonon dispersion relations in high-symmetry directions, with accompanying density of states plots, for a bulk zinc-blende cadmium selenide system. (a) VASP GGA DFT results. (b) VFF using no atomic charge. (c) VFF using the DCM.

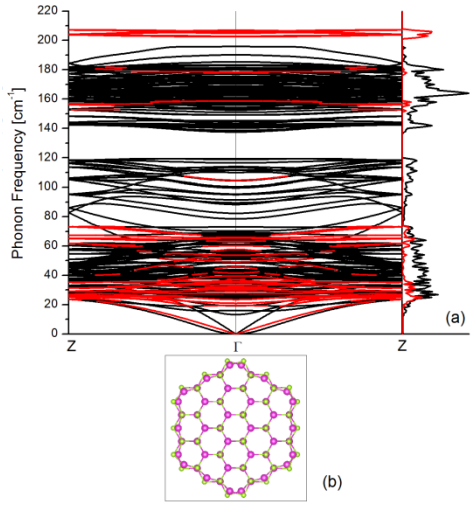

FIG. 8. (a) Phonon dispersion along the z-axis, with accompanying density of states plot, for a wurtzite CdSe nanowire with cross section shown in (b) (cadmium atoms in purple, selenium atoms in green). A VFF potential with the DCM, fit to the slab CdSe system of Fig.6 is used here. Phonon eigenstates to which the outermost layer of atoms contributes at least 51% are colored in red, and their collective contribution to the density of states is plotted in red along with the total DOS (in black).